5. Hydration studies

This section serves two purposes. On the one hand, it provides examples of the general concepts introduced in the preceding sections and on the other hand, it presents additional methods and technical problems which are best discussed in context with NMR hydration studies. Representative examples of experiments are used to discuss the specific technical problems encountered when using NMR for studies of hydration.

5.1 Hydration

Interest in the hydration of proteins arises from a desire to understand the influence of water on the structural, functional, and dynamic properties of biological macromolecules such as proteins. Despite their importance the details of water–protein interactions are not well understood. The compact folding of the polypeptide chains in globular proteins usually excludes the solvent from the molecular core leading to a hydration shell constituting the interface between solvent and molecules dissolved. Still a small number of water molecules in the interior of proteins are often observed in single crystals [221]. These are typically completely shielded from the bulk solvent, form hydrogen bonds with surrounding polar groups of the polypeptide chain, and are thus an integral part of the protein architecture. Similar data to those for interior water molecules in globular proteins in solution have been reported for the intermolecular interfaces in multimolecular complexes with proteins, for example, in protein–DNA complexes [222, 223].

Crystal structures of proteins report the position of some hydration water molecules in the interior as well as on the surface of the molecules. However diffraction experiments probe only the total fraction of time that a particular hydration site is occupied by a water molecule; they are insensitive to the residence time at that site for a particular water molecule. The lack of experimental methods to determine the dynamic behaviour of water molecules at individual sites at the protein-water interface has prevented a more detailed understanding of hydration. This situation improved in the last few years with the development of NMR techniques enabling studies of individual hydration sites providing both structural data at atomic resolution and information on dynamic aspects of biomolecular hydration [224].

5.2 NMR and hydration

The potential of NMR to contribute to the understanding of hydration was realized a long time ago. In 1963 it was observed that proteins dissolved in water increased the relaxation rates of the protons in water. This was shown to be due to an increase of the correlation time of a fraction of the water molecules [225]. The interpretation of this data left two possible explanations. Either a very small number of water molecules stick to the protein for a time much longer than the rotational correlation time τ_R of the protein or hundreds of water molecules have a residence time on the order of τ_R [226]. The controversy could only be resolved when a new class of NMR experiments was developed that uses cross relaxation (NOE/ROE) between protons in water molecules and protons of the protein [227]. The NOE and ROE are proportional to the inverse sixth power of the distance between the protons and further related to a correlation function describing the stochastic modulation of the interaction (Eq. (2.13), Eq. (2.16)). For studies of hydration, it is important that this correlation function may be governed either by the Brownian rotational tum-

bling of the hydrated molecule or by interruption of the dipolar coupling through translational diffusion of the interacting spins.

The application of NMR hydration experiments to the bovine pancreatic trypsin inhibitor (BPTI) revealed two distinguishable classes of hydration water molecules in aqueous protein solutions [228–230] (Fig. 29): interior hydration and surface hydration water molecules. Interior hydration

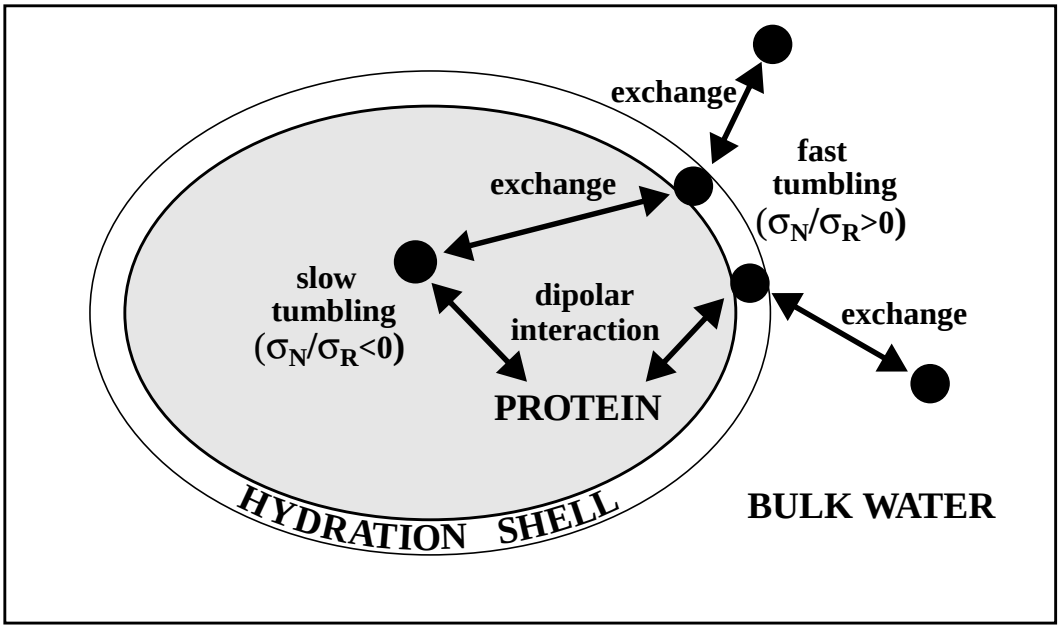

Fig. 29. Schematic representation of a protein shown as a grey ellipse with its hydration shell in an aqueous solution. Black circles represent individual water molecules. Three types of water molecules can be distinguished: bulk water molecules which do not interact with the protein, water molecules in the surface hydration shell which weakly interact with the protein and water molecules in the interior of the molecule. Surface hydration water molecules and interior water molecules show dipolar interactions with the protein and can be distinguished by the different signs of their ratio between the ROE and NOE cross relaxation rates σ_R and σ_N.

waters show cross relaxation with nearby polypeptide protons which is in the slow motional regime. This motional regime is distinguished by opposite signs of the cross relaxation rate constants in the laboratory frame of reference, σ_N (Eq. (2.13)), and in the rotating frame, σ_R (Eq. (2.16)). Such water molecules have a ratio $\sigma_N/\sigma_R < 0$ indicating lifetimes with respect to exchange with the bulk water greater than 10^{-9} s. Surface hydration waters, however, have a ratio $\sigma_N/\sigma_R > 0$ and much smaller exchange life times in the approximate range of 10^{-11} to 10^{-9} s. Similar data to those for interior hydration of globular proteins in solution have been obtained from NMR studies of the intermolecular interface in complexes between a protein and a DNA duplex [223]. Detailed descriptions of applications of NMR to study hydration can be found in recent reviews [231–233].

Compared to surface hydration waters interior hydration waters give much more intense NOEs with the protons of the protein because of their longer residence times. However the residence times are still short enough to observe the same ^{1}H chemical shifts for the interior waters and the

bulk water due to exchange averaging [202, 229, 234]. Not only water molecules exchanging with the hydration shell resonate at the water frequency but any fast exchanging proton of the protein, especially hydroxyl protons. Consequently NOEs between these protons and other protons of the protein are indistinguishable from NOEs with water. This degeneracy requires that complete proton assignments are available for the protein and that the solution structure is known to distinguish NOEs to hydration water molecules from these rapidly exchanging protons of the protein. In contrast to the hydroxyl protons in the amino acids Ser, Thr and Tyr the carboxylic acid proton of the Glu and Asp side chains and the C-terminus do not interfere with hydration measurements [235].

Surface hydration water molecules which show NOEs to protons of a protein with positive σ_N can be detected without the ambiguity introduced by exchanging protons. None the less they suffer from the interference with exchanging protons since they become undetectable when their weak NOE signal overlaps with a strong peak of an interior or exchanging proton. Hence for proteins with interior water molecules and/or with a considerable number of hydroxyl protons, a complete hydration shell cannot be observed.

The methods developed for hydration measurements can also be used to study the interaction of proteins with other small molecules. The investigation of ligand binding sites [236] and the interaction with denaturants is of special interest in this context [237]. Not only native proteins but also proteins in a denatured state can be studied [238] which do not have a well defined structure even though structured parts may transiently form [239]. Sequential assignments are a prerequisite for solvent-protein interactions by NMR and can be obtained in the denatured state using isotope labelled proteins [215, 240, 241].

5.3 Basic experiments

5.3.1 NOEs between water and protein protons

The first experiment for the observation of individual hydration sites of proteins was a NOESY where the water line was not suppressed before the mixing time but only just before acquisition of the data [227]. With this method water and protein protons will cross relax during the mixing time when the interproton distance is not larger than about 0.4 nm [227]. Fig. 30 shows a NOESY pulse sequence that would typically be used to study hydration. After the excitation pulse on all protons a pair of gradients prevents radiation damping of the water resonance during the evolution period [90] (Fig. 22E). During the NOE mixing period τ_m (Fig. 15A) which is embraced by two 90^o pulses a gradient keeps the water magnetization along the *z* axis and destroys all single and multiple quantum coherences present during τ_m (Fig. 22A). Finally, the water resonance has to be removed to prevent overload of the receiver. The scheme in Fig. 30 utilizes the WATERGATE sequence for this purpose (Fig. 28C). The use of *rf* gradient pulses as originally proposed for water suppression may transfer magnetization *via* the TOCSY or ROESY effect already for very short durations of the trim pulses [73]. The application of the pulse sequence results in a 2D NOESY spectrum (Fig. 31) where the cross section through the water resonance parallel to the frequency axis ω_2 contains all interactions between water and protein protons. These interactions include intermolecular NOEs between water and protein protons, intramolecular NOEs between protons of the protein where one nucleus resonates near the water frequency and exchange peaks between labile protons and water. The spectrum in Fig. 31 was recorded with the protein BPTI,

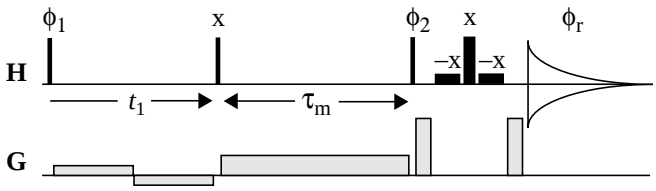

Fig. 30. Pulse sequence for the detection of intermolecular NOEs between water molecules and protein protons using the phases indicated above the pulses and the following phase cycles: ϕ_1 = x, –x; ϕ_2= x, x, –x, –x; ϕ_r = x, –x, –x, x. During the evolution period t_1 and the mixing time τ_m gradients are applied to prevent radiation damping (Fig. 22A and Fig. 22E). Just before acquisition a WATERGATE sequence (Fig. 28C) is used to destroy the water magnetization.

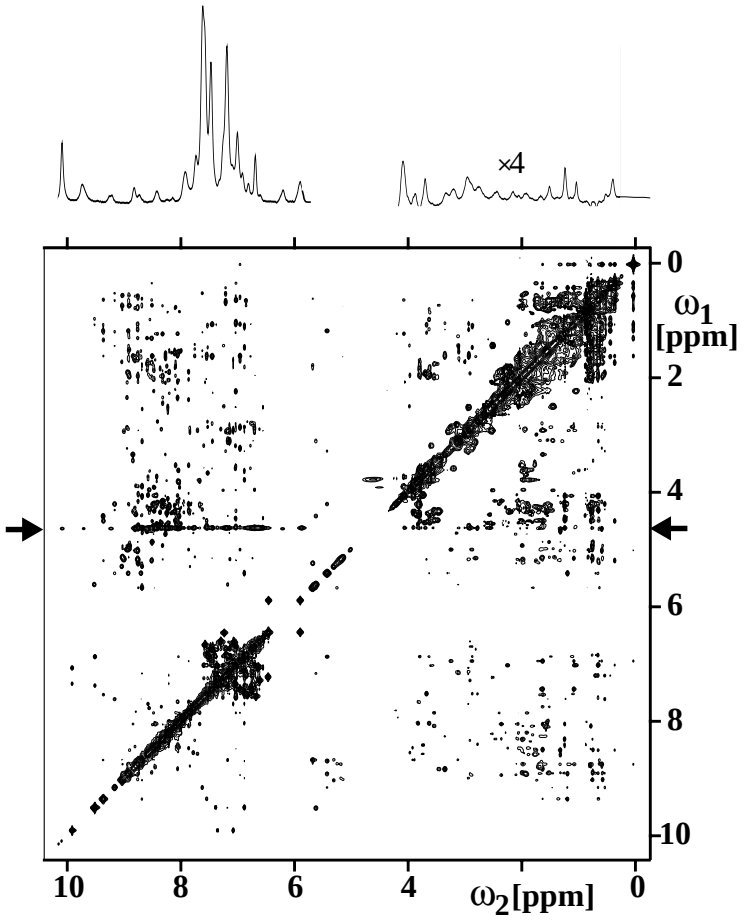

Fig. 31. 2D NOESY spectrum of 10 mM BPTI in a solution of 90% H_2O/10% D_2O at 277K obtained with the pulse sequence shown in Fig. 30. The horizontal cross section containing the interactions between protons of the water molecules and protein protons is indicated by arrows and plotted above the 2D spectrum. The spectral range from 0 to 4 ppm in the cross section is expanded in the vertical direction by a factor of 4 compared to the spectral region from 6 to 10 ppm which is dominated by strong exchange peaks. Exchange peaks and NOEs to the four interior water molecules of BPTI dominate the cross section and weak NOEs to surface hydration water molecules are only visible for a few methyl groups around 0.6 ppm.

which contains four interior water molecules [227]. In a horizontal cross section through the water line the different resonances cannot be unambiguously assigned and overlap between positive and negative resonances cancels the very small contributions from the rapidly exchanging surface hydration water molecules. NOEs to interior water molecules and exchanging protons of the protein result in positive peaks which dominate the cross section shown in Fig. 31. Very few interactions with surface hydration water molecules are observable around 0.6 ppm (negative peaks) even though potentially all protein protons on the surface should show an interaction with water. To avoid extensive overlap the resonances representing the interactions have to be resolved into an additional dimension by some transfer element (Section 4.2). Expanding the NOESY sequence into a 3D experiment results in a 2D cross section through the water line which contains all resonances of interest. An analogous result can be more efficiently obtained if the water is selectively excited which results in a 2D spectrum. There are a number of schemes that excite water more or less selectively [73, 202, 242–248]. All but one sequence [73] suffer from a technical limitation that is quite common in NMR spectra of macromolecules: the water line and some protein resonances usually overlap, which makes the distinction between water-protein interactions and intraprotein NOEs difficult for protons resonating near the water line. Even in uniformly [^{15}N,^{13}C]-isotope enriched proteins where intramolecular NOEs can be suppressed using ^{15}N- and ^{13}C-filtering techniques [143], there remains a risk of "breakthrough" of intramolecular NOEs unless the level of enrichment reaches 100% [249].

5.3.2 HYDRA

The HYDRA experiment [73] strictly selects only water-protein interactions even if protein resonances overlap with the water line. These interactions include NOEs as well as chemical exchange. In HYDRA the separation of intermolecular solvent-protein NOEs from intramolecular NOEs is based on the different diffusion constants of water molecules and the biological macromolecules. As a rule, water molecules diffuse about 15 to 25 times faster than proteins in the molecular weight range $10-20$ kDa. On this basis, intermolecular water–protein NOEs can be distinguished from intramolecular NOEs with the use of the diffusion segment shown in Fig. 21 which is often referred to as a diffusion filter [203]. A suitably designed experiment which measures the difference between the signals obtained with strong and weak PFGs in a diffusion filter, selectively records intermolecular protein–water interactions. Fig. 32 shows the pulse sequence for a 1D HYDRA experiment. HYDRA consists of a NOE or ROE mixing period sandwiched between two diffusion filters. The spectrum containing only water–protein interactions is obtained taking the difference between the data measured in alternating scans using the gradient traces G_I and G_{II}, respectively. The delay Δ and the gradient strengths G_1 and G_2 are chosen such that G_1 destroys most of the water magnetization due to its rapid diffusion (Eq. 4.4)), whereas G_2 destroys only a small amount of the water magnetization. Subtraction of the two measurements I and II cancels intramolecular Overhauser effects whereas intermolecular interactions between water and protein protons are retained. For the suppression of the residual water before acquisition, the second diffusion filter is combined with a WATERGATE sequence [87] (Fig. 28C). Compared to techniques based on selective excitation, the introduction of diffusion filters reduces the sensitivity [73]. None the less HYDRA will probably be the method of choice whenever suppression of intramolecular NOEs is important. HYDRA can be used with very short ROE or NOE mixing times. This is in contrast to some schemes using radiation damping [246], where mixing times of less than 60 ms cause severe loss in sensitivity and/or in selectivity of the water excitation. Use of very short mixing times may be necessary for studies of short lived surface hydration, since the very weak NOEs between protein protons and surface hydration water would

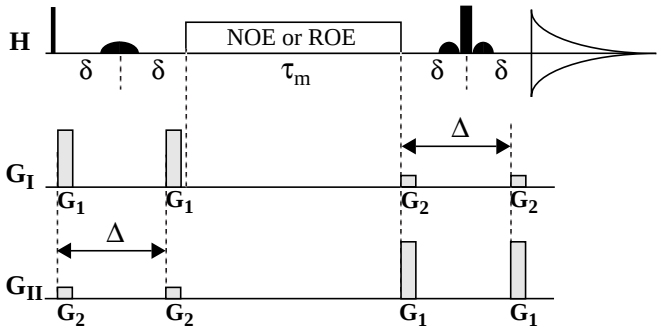

Fig. 32. Schematic experimental scheme for HYDRA difference experiments with diffusion filters for the separation of intermolecular and intramolecular interactions between protein and solvent protons. The curved shapes on the line *H* indicate selective pulses at the water frequency. For the NOE or ROE mixing during τ_m the transfer segment for NOESY or ROESY shown in Fig. 15 must be inserted. The lines G_I and G_{II} indicate the applied magnetic field gradients; the desired spectrum corresponds to the difference between two subsequent experiments recorded with G_I and G_{II}, respectively. The duration of the diffusion filter is 2δ and Δ is the diffusion time. The second diffusion filter immediately before acquisition is combined with a WATERGATE sequence (Fig. 28C) to suppress the water resonance. The HYDRA experiments with NOE or ROE mixing have a different phase cycling scheme that provide optimal subtraction of unwanted resonances [73].

otherwise be masked by overlap with much stronger NOEs originating from spin diffusion with interior water molecules or labile protein protons (Fig. 31).

As with any difference experiment HYDRA requires special attention to obtain no subtraction artifacts. For this reason the water resonance in the first diffusion filter is refocused by a selective 180^o pulse, so that only macromolecular resonances close to the water are preserved and most of the protein magnetization is destroyed before the mixing time (Fig. 22D). This improves the quality of the experiment since for example methyl resonances can no longer create subtraction artifacts which is a common limitation in difference experiments. When working with macromolecules the duration of the diffusion filter should be kept as short as possible to minimize signal loss due to relaxation. This requires strong gradients that may interfere with the performance of the experiment since two different gradient schemes G_I and G_{II} are used which induce different transient effects. Shaped gradients with a smooth rise and fall minimize these transient effects and reduce the artifacts in the difference spectrum. One possibility is a modified rectangular shape with the first quarter having a sine-squared and the last quarter a cosine-squared dependence [68, 202]. In HYDRA experiments with a NOE mixing period the same amount of magnetization from protein protons has relaxed after τ_m for both gradient sequences G_I and G_{II}. Due to the different strengths of G_1 and G_2 in the second diffusion filter, this would result in a non-zero difference spectrum. Since the NOE depends only on population differences the water magnetization can be flipped into the positive and negative *z* direction at the start of the mixing time, which allows subtraction of the residual difference caused by the relaxed protein magnetization. For the experiments with a ROE mixing time there is no relaxed magnetization after the spin-lock mixing and no compensation is necessary.

To achieve the spectral resolution needed for obtaining individual assignments of water–protein

interactions, the basic 1D HYDRA scheme (Fig. 32) can be combined with any transfer element (Section 4.2) to generate a higher-dimensional experiment. Fig. 33 compares a 2D [^{1}H,^{1}H]-TOCSY-relayed HYDRA spectrum [73] with a 2D [^{1}H,^{1}H]-TOCSY-relayed NOE experiment

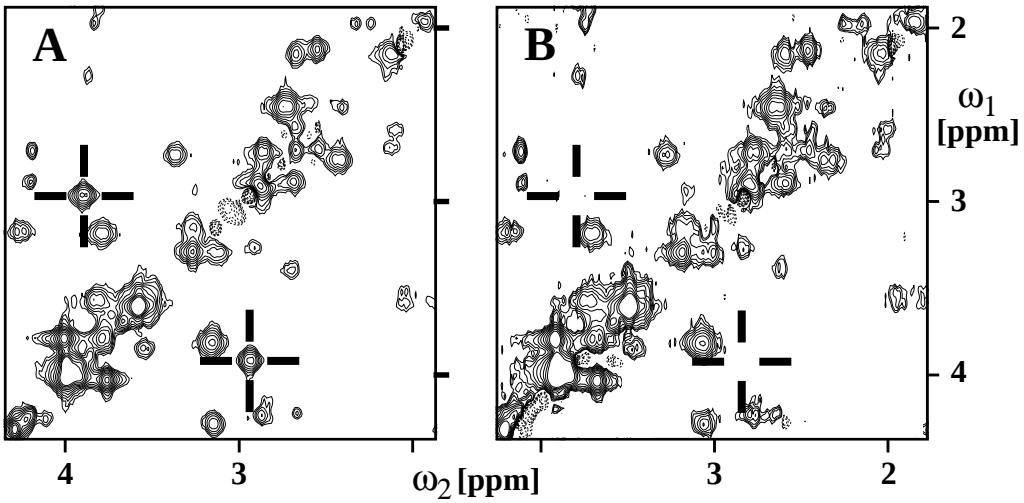

Fig. 33. Contour plots of expansions of 2D TOCSY-relayed NOE difference spectra measured with a 20 mM solution of BPTI at a temperature of 277 K. The solvent was 90% H_2O/10% D_2O at pH 3.5. The NOE and the TOCSY mixing times were 60 ms and 27 ms, respectively. The crosses mark the position of the TOCSY-relayed intramolecular NOE between Cys 38 H^{α} and Cys 38H^{β}. (A) [^{1}H,^{1}H]-TOCSY-relayed NOE difference spectrum using radiation damping for the selection of the water resonance. (B) [^{1}H,^{1}H]-TOCSY-relayed HYDRA experiment. The intramolecular NOE Cys 38 H^{α}/Cys 38H^{β} is suppressed and the remaining TOCSY-relay peaks indicate intermolecular NOEs to interior water molecules or rapidly exchanging protons of the protein.

which uses radiation damping for the water selection [250]. The diagonal in these 2D spectra comprises peaks which originate from NOEs or chemical exchange between water and protein protons. The TOCSY segment transfers magnetization from the diagonal peaks to scalar coupled protons resulting in a cross peak at the same ω_1 frequency as the diagonal peak. The spectra were recorded with a solution of the protein BPTI. The positive cross peaks correspond to signals that were previously assigned either to NOEs with the four interior water molecules in BPTI, to exchange peaks or to NOEs with rapidly exchanging side chain hydroxyl protons of the protein [251]. The spectral region shown does not contain negative cross peaks which would indicate NOEs between water protons and solvent accessible protons on the protein surface. Either their signal intensity is too small to be detected or they overlap with strong positive peaks. In Fig. 33A the spectrum collected using radiation damping to selectively excite the water contains a TOCSY-relayed NOE between Cys 38 H^{β} and Cys 38 H^{α} (marked by a cross), because the chemical shift of the Cys 38 H^{α} resonance coincides with that of the solvent water resonance. The HYDRA spectrum of Fig. 33B contains exclusively interactions with water protons, as is demonstrated by the absence of the cross peak between Cys 38 H^{β} and Cys 38 H^{α}.

5.3.3 Measurement of exchange rates using diffusion filter experiments

Observation of hydration water molecules located in the core of globular proteins by NMR spectroscopy showed that these have ^{1}H chemical shifts identical with that of the bulk water, implicating exchange averaging of the shifts in the two environments [229]. The exchange rates for the interior hydration sites is of interest since these can be directly related to the frequency of internal motions of the protein. However measurements of fast exchange rates in the expected range of 10^3 s^{-1} to 10^6 s^{-1} are rather difficult. Two techniques have been proposed to determine the exchange rates or residence times of interior water molecules. One method uses the dependence of ^{17}O and ^{2}H relaxation in water molecules on the main magnetic field and allows determination of residence times τ_{res} in the range from 4 μs to 200 μs [226, 252, 253]. The other method is based on diffusion weighted NOESY experiments [202, 242] and current technology permits to measure minimal values for τ_{res} of 1 ms. Although the following discussion of the latter method concentrates on the measurement of residence times of interior water molecules, the same technique can be used for the determination of fast exchange rates, for example of rapidly exchanging hydroxyl or amide protons with the bulk water.

In a suitably designed NOESY experiment with a diffusion filter the decaying signal amplitudes of protein resonances will record *via* their NOEs the diffusion properties of the otherwise unobservable interior water molecules. The average translational diffusion constant for water molecules transiently trapped inside macromolecules is smaller than for bulk water. This difference reflects the lifetimes of the interior water molecules. Fig. 34 shows a pulse sequence used

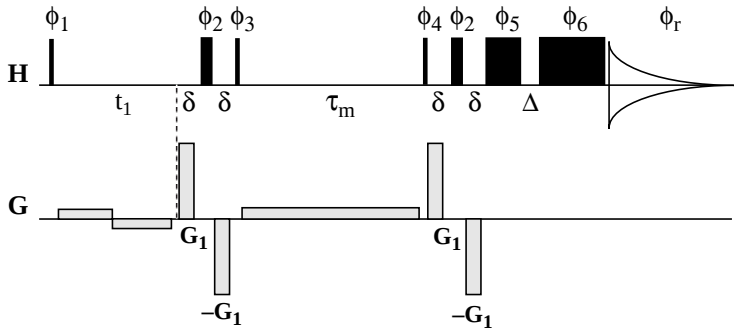

Fig. 34. Experimental scheme for a 2D [^{1}H,^{1}H]-NOESY used to measure exchange rates based on the different translational diffusion of water and macromolecules. On the horizontal line labelled H *rf* pulses applied at the resonance frequency of protons are indicated and on the line G the position of PFGs is shown. The evolution time is t_1, τ_m the NOESY mixing period and δ a short delay of 1 ms or less for the application of the very strong magnetic field gradients G_1. A weak gradient is used to destroy unwanted magnetization during τ_m. Immediately before acquisition two spin-lock purge pulses separated by the duration Δ are applied to suppress the water resonance (Fig. 28B). The phase cycle is as follows: ϕ_1 = 8(x), 8(–x); ϕ_2 = 2{2x, 2y, 2(–x), 2(–y)}; ϕ_3 = 8{x, (–x)}; ϕ_4 = 4{2(x), 2(–x)}; ϕ_5 = 16(y); ϕ_6 = 2{4x, 4(–x)}; with the receiver cycle ϕ_r = 2{x, 2(–x), x}, 2{–x, 2x, –x}. Quadrature detection in t_1 is achieved by altering the phase ϕ_1 according to States-TPPI (Table 3).

for the measurement of lifetimes of interior water molecules [202]. The addition of pulsed magnetic field gradients, which are applied before and after the mixing time, τ_m, introduces diffusion rate dependent signal intensities of the NOEs between protons in water molecules and protein protons. Self-compensating "PFG sandwiches" [68] are used instead of single gradient pulses to reduce unwanted transient distortions. This allows much shorter recovery times than would be

possible with a single magnetic field gradient. During the evolution time t_1 very low amplitude PFGs are applied which defocus and refocus the desired magnetization while preventing radiation damping [90] (Fig. 22E). Another low amplitude PFG during the mixing time eliminates coherences present after the second 90^o *rf* pulse. Water suppression is achieved just prior to acquisition by a pair of orthogonal trim pulses separated by a short delay Δ [77, 250] (Fig. 28B). In addition these trim pulses select magnetization components along the *x* axis only which results in a phase sensitive spectrum [208]. For the determination of the exchange rates, a series of spectra with increasing gradient strength G_1 is measured. The shortest exchange lifetime that can be determined depends on the largest available gradient strength [202]. Measuring a life time of about 1 ms requires a gradient strength of 2 T/m which is technically very demanding. The goal to measure even shorter lifetimes can only be reached by the use of shorter and stronger gradients with extremely brief gradient recovery times. With such an improved gradient hardware, measurements of residence times of interior water molecules in the submillisecond range will become possible.

The experimental scheme in Fig. 34 was used to measure the residence time of interior water molecules in BPTI [202] which contains four interior water [254, 227]. A maximal lifetime of 10^{-3} s could be established for both, the cluster of three water molecules, which is partly surface accessible and a completely buried single water molecule. The limit of 10^3 s^{-1} is set by the maximal available gradient strength of 1.8 T/m. The result indicates, that motions with amplitudes of approximately 0.15 nm must occur with a frequency of at least 10^3 s^{-1} even in the core of a small protein.

5.3.4 Relaxation Dispersion Experiments

In relaxation dispersion experiments average relaxation properties of nuclei in water molecules are measured in aqueous protein solutions. The deviation of this average relaxation from relaxation in pure water samples describes the influence of hydration water molecules. The relaxation behaviour of hydration water molecules differs from bulk water molecules due to their different mobility which is reflected in different correlation times [225]. For a systematic investigation of molecular motions of hydration water molecules by relaxation rate measurements, it is necessary to investigate the frequency dependence of the relaxation over an extended resonance frequency range. Such measurements with aqueous protein solutions were first performed almost 30 years ago [252] and were referred to as nuclear magnetic relaxation dispersion experiments. Details on the techniques used can be found in a review on dispersion or field cycling experiments [255]. In contrast to NOE based experiments the results of relaxation dispersion measurements cannot directly be assigned to individual hydration sites nor can independent information be derived on the number and lifetimes of hydration waters.

Although nuclear spin relaxation dispersion of the nuclei ^{1}H, ^{2}H, and ^{17}O in water molecules has long been recognized to contain dynamic information on the interaction of water with proteins in aqueous solutions the interpretation of the data has been controversial. Only recently it was proposed that most of the ^{17}O relaxation dispersion could be due to interior water molecules [256]. For ^{17}O the dominant relaxation process is based on quadrupolar interactions with electric field gradients. Qualitatively ^{1}H and ^{2}H show a similar relaxation dispersion curve to that of ^{17}O but their relaxation is affected by hydrogen exchange. In addition the interpretation of ^{1}H relaxation suffers from cross-relaxation between protein and water protons [257, 258]. The determination of the contribution of the interior water molecules to the relaxation dispersion of ^{1}H and ^{2}H requires

measurements at different pH/pD values, the knowledge of all pK values, all exchange rate constants and for protons in addition the relevant cross relaxation rates [231, 253, 258, 259]. Often this data is not available to the degree of completeness required for a detailed analysis of ^{1}H and ^{2}H relaxation dispersion data. Typically only a few interior water molecules contribute to the relaxation dispersion and, hence, even a small number of rapidly exchanging protein deuterons or protons can make a contribution to the dispersion comparable to that of all interior water molecules.

Fig. 35 shows representative relaxation dispersion curves of ^{17}O and ^{2}H in water molecules obtained for aqueous protein solutions; relaxation rates are plotted versus $\omega\tau_c$ where ω is the Larmor frequency and τ_c the correlation time of the water molecules. The longitudinal, T_1^{-1}, and the transverse, T_2^{-1}, relaxation rates show a frequency dependence for values of $\omega\tau_c$ in the range from 0.1 to 10 which correspond to resonance frequencies in the range of 1 to 100 MHz. At low frequencies the two relaxation rates are equal if the pH of the solution is either low or high, for a pH close to neutral there is a further dispersion at a frequency of a few kHz [255, 260] due to proton exchange between different water molecules. At high frequency the dispersion curves still deviate from the relaxation rate of bulk water. A further dispersion is expected at even higher fre-

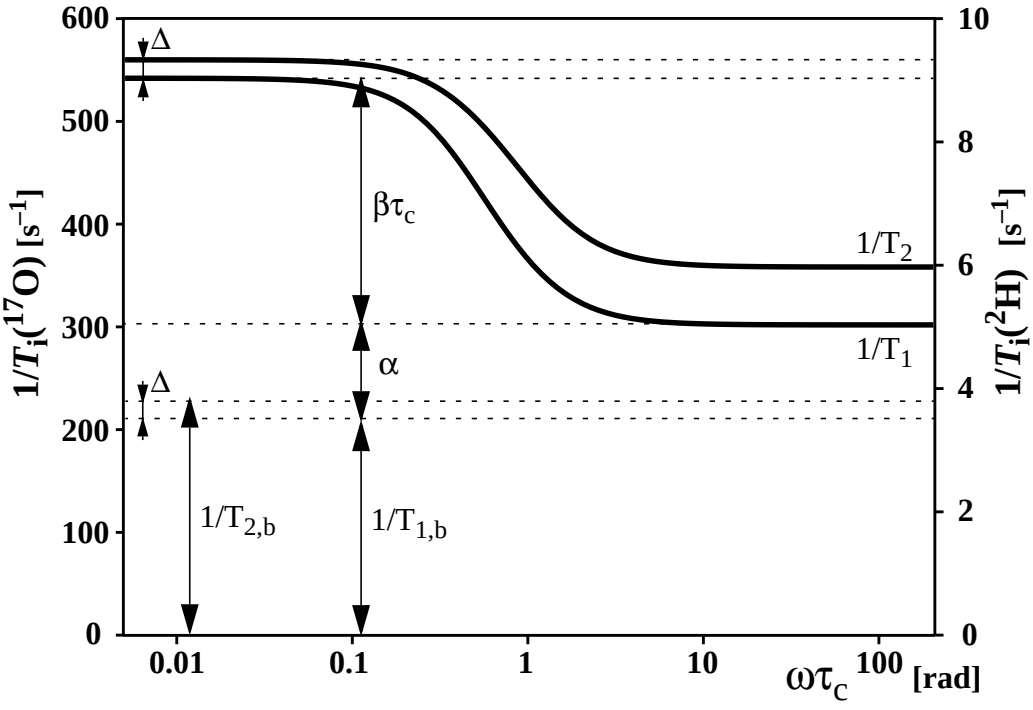

Fig. 35. Typical relaxation dispersion obtained when measuring the field dependant longitudinal, $1/T_1$, and transverse, $1/T_2$, relaxation rates of ^{17}O and ^{2}H nuclei in water molecules in an aqueous protein solution. The relaxation rates are plotted against the product of the Larmor frequency ω and the rotational correlation time τ_c of the water molecules. The variables α and β describe the two plateaus reached at small and large values of $\omega\tau_c$. The frequency independent relaxation rates of bulk water are indicated by $1/T_{i,b}$ with i being 1 or 2. The difference between the two rates at low frequency is indicated by Δ.

quencies containing information on the interaction of water molecules with the surface of the protein. The general functional form of the longitudinal relaxation for Larmor frequencies from about 0.1 to 1000 MHz can be described by Eq. (5.1) [261].

$$1/T_1(\omega) = 1/T_{1,b} + \alpha + \beta\,[\tfrac{1}{2}J(\omega) + 2J(2\omega)] \qquad (5.1)$$

$T_{1,b}$ is the frequency independent longitudinal relaxation time of the bulk water. The parameters α and β are illustrated in Fig. 35 and the spectral density function $J(\omega)$ is given in Eq. (2.8). The parameter Δ in Fig. 35 describes the additional transverse relaxation which is due to a modulation of the only partially averaged scalar coupling between the hydrogen atom and ^{17}O. This scalar relaxation of the first kind depends on the pH and can be neglected for pH values below 4.5 and above 9.5 [260]. The value for Δ reaches a maximum around neutral pH with typically 0.6 s^{-1} for protons and 250 s^{-1} for ^{17}O. The parameters α and β have been attributed to the water molecules interacting weakly and those interacting strongly with the protein [226]. In this interpretation α describes the surface hydration water molecules and the term β relates to the interior water molecules with a residence time longer than the rotational correlation time τ_R of the molecule. The term α describes average properties of a large number of surface water molecules and is more difficult to analyse than β [226]. Thus the interpretation of relaxation dispersion measurements focuses on β which depends only on a few interior waters and in some cases allows the characterization of individual binding sites for interior water molecules. For ^{17}O relaxation the dominant contribution to β originates from quadrupolar relaxation. This is not the case for ^{1}H and ^{2}H relaxation where exchange contributions may dominate. Measurements with BPTI show a strong pD dependence of the term β [253] for ^{1}H and ^{2}H relaxation.

Eq. (5.1) has the same dependence on the spectral densities as quadrupolar relaxation [29]. The explicit functional form of the spectral density functions in Eq. (5.1) depends on the time correlation function of the fluctuations relevant for relaxation and on the shape of the protein. If rotational diffusion of a spherical protein is assumed the spectral densities given in Eq. (2.8) are obtained. In this case a simple relation between the Larmor frequency at which half the maximum relaxation dispersion is reached, $\omega_{1/2}$, and the correlation time τ_c is obtained with $\tau_c = \sqrt{3}\omega_{1/2}$ [252]. Only waters that exchange with a residence time τ_{res} longer than the rotational correlation time of the protein (typically 5 ns or longer) feel the Brownian motion of the macromolecule and contribute to the relaxation dispersion. On the other hand the average relaxation of the bulk water can only be enhanced by exchange into the protein interior if τ_{res} is shorter than the interior water spin relaxation time which is about 4 μs for ^{17}O and 200 μs for ^{2}H [253]. Thus for a medium sized protein the maximal residence time measurable by relaxation dispersion experiments is about 2.5 μs for ^{17}O and 75 μs for ^{2}H. Since ^{2}H relaxation is slower than ^{17}O relaxation, a comparison of ^{2}H an ^{17}O relaxation data may reveal interior water molecules which exchange too slowly to influence the ^{17}O relaxation [253].

The experimental implementation of relaxation dispersion measurements is based on simple pulse sequences. The sensitivity of experiments measuring ^{17}O relaxation is greatly improved by using water enriched in ^{17}O isotopes from natural abundance of 0.037% to a level of about 20%. Longitudinal relaxation rates are often measured by the inversion-recovery pulse sequence (180-τ-90) and transverse relaxation rates by the spin-echo experiment (90-τ/2-180-τ/2). Both experiments are measured for an array of different values of τ and at different magnetic field strengths. For a good representation of the relaxation dispersion curve, relaxation for values of $\omega\tau_c$ between 0.05 and 20 should be measured (Fig. 35). Thus experiments for a medium size protein with a correlation time of 10 ns require measuring at different magnetic fields where the resonance fre-

quencies of the respective nucleus vary in the range from 0.8 to 320 MHz. In practice the accessible range is more restricted due to the small sensitivity at low frequencies and the available magnetic field strength at high frequencies. Missing relaxation rates at high and at low resonance frequencies limit the precision of the determination of the plateaus reached at these two extremes (Fig. 35) and thus the precision of the parameters α and β. The relaxation dispersion of the transverse relaxation time can be used to confirm that the low frequency plateau is reached in cases where Δ in Fig. 35 is zero.

Very extensive relaxation dispersion data have been collected for BPTI and a BPTI mutant lacking one interior water. The measurements extended over all the three nuclei ^{17}O, ^{2}H and ^{1}H and residence times of the four interior water molecules in native BPTI were determined to lie in the range from 0.01 μs to 1 μs for three waters and at 170 μs for the fourth water at a temperature of 300K [262]. Comparison of the relaxation dispersion data for native BPTI and that of the mutant showed that the most deeply buried water molecule has a residence time which is too long to influence the ^{17}O relaxation in the measurement conditions used [234]. The work with BPTI demonstrated that not only the precise 3D structure with the known positions of interior water molecules but also the use of mutants may contribute to an assignment of the different contributions to relaxation by interior water molecules at individual sites.

The two techniques using relaxation dispersion or diffusion weighted NOESY spectra [202] (Section 5.3.3) are complementary and make NMR a powerful tool for the investigation of residence times of interior water molecules.

5.4 Artifacts in hydration studies at high magnetic fields

5.4.1 Radiation damping and demagnetizing field effects

The use of high magnetic fields and the improved sensitivity of probes increases the interference of the magnetization of protonated solvents, for example water, with the performance of the experiment. Usually, the magnetic field in a NMR sample is assumed to be constant during a NMR experiment. However, variations of the longitudinal component of the solvent magnetization during a pulse sequences may induce small changes of the magnetic field [94]. During a typical NMR experiment the magnetic field introduced by the solvent magnetization is time-dependent, which causes a nonlinear behaviour of the system. One consequence of the changing longitudinal solvent magnetization is alteration of the precession frequencies of all nuclei in the sample. Two effects are associated with the water magnetization: radiation damping and the demagnetizing field. In this section consequences of the two effects are presented using as an example experiments applied to studies of macromolecular hydration.

Radiation damping is a well known effect in high resolution solution NMR, which rotates the solvent magnetization back to the external magnetic field direction *via* the coupling of the magnetization with the resonant circuit of the detection system [263]. This behaviour can be represented as an induced shaped radio-frequency pulse (Fig. 36). The radiation damping field is commonly assumed to affect signals only in a narrow frequency range close to the solvent resonance, but it can influence signals with resonance frequencies differing by several kHz from that of the solvent signal in spite of its small strength of 15 – 30 Hz. The amplitude, phase and frequency of such

signals can be disturbed giving rise to spectral artifacts. In particular when difference methods are used to obtain the final spectrum, the spectral quality may suffer severely due to such artifacts.

The demagnetizing field in an NMR sample is caused by highly abundant species of the solvent protons in aqueous solutions of proteins. The magnetization of the water protons at high magnetic fields becomes large enough to measurably influence the magnetic field in the sample. As a consequence the resonance frequencies of all spins change slightly depending on the state of the solvent magnetization. The strength of the demagnetizing field depends on the sample geometry and vanishes completely in a spherical sample [94]. Unfortunately this is not a practical alternative to cylindrical NMR tubes and results in reduced sensitivity. The largest chemical shift difference is obtained with the solvent aligned along the positive and the negative *z* axis and reaches about 2 Hertz for protons at 750 MHz in a standard cylindrical sample. The terms “dipolar field” [264] and “bulk susceptibility effect” [94] are alternatively used to denote the same effect. The most direct influence can easily be envisaged in difference experiments in which the water magnetization has a different state in alternate scans which are subtracted from each other.

5.4.2 Minimizing artifacts in hydration measurements

NMR pulse sequences for hydration studies must be designed for the detection of very weak signals in the presence of very intense solvent lines. This has been achieved with the use of selective excitation techniques, the exploitation of radiation damping, isotope filtering and differential diffusion or differential relaxation properties [73, 202, 242–248]. In many cases, the NMR experiments for studies of macromolecular hydration make use of difference techniques, and are therefore particularly prone to deterioration by artifacts originating from specific NMR properties of the solvent, such as radiation damping and the nuclear demagnetizing field.

The pulse sequence used to demonstrate the influence of radiation damping and the demagnetizing field effect on hydration studies is shown in Fig. 36. This 2D {^{15}N,^{1}H}-HSQC-relayed NOE difference experiment derives from a scheme described previously [73, 95]. The first scan labelled (I) uses radiation damping to rotate the water magnetization back to the equilibrium direction after the 90^{o} pulse labelled b. All remaining transverse magnetization after the NOE mixing time τ_m is dephased by the gradient G_2. In the second scan labelled (II), all transverse magnetization is dephased immediately after the 90^{o} pulse b by an additional gradient G_2 which prevents radiation damping. The difference spectrum obtained from these two scans contains water–protein NOEs, exchange peaks with water, and possibly HN–C$^{\alpha}$H NOEs when C$^{\alpha}$H chemical shifts are close to that of water. To prevent artifacts originating from non-steady state conditions, the scheme starts at position a with the sequence G_1 – 90^{o}(^{1}H) – G_1 to dephase all proton magnetization (Fig. 28F).

NOEs between surface hydration water molecules and the protein are very small making experimental schemes used for such studies especially sensitive to artifacts. Thus the robustness to artifacts must be tested for all pulse sequences used in hydration experiments. A first test applies solvent presaturation prior to the sequence and must result in a spectrum which contains no NOEs between solvent protons and protein protons. A further test appropriate for the experiment in Fig. 36 requires perfect subtraction of the signals in the {^{15}N,^{1}H}-HSQC relay step alone. Perfect cancellation for the relay step documents that the stability of the spectrometer is sufficient, the magnetic field gradients used do not create artifacts, the parameters of the field-frequency

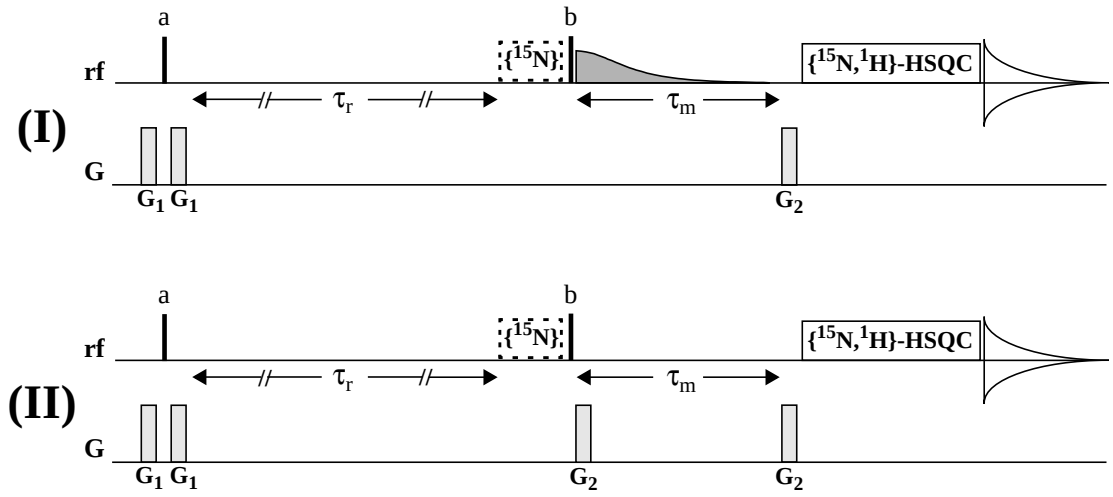

Fig. 36. Schematic pulse sequence for a 2D {^{15}N,^{1}H}-HSQC-relayed NOE difference experiment for protein hydration studies [73, 95]. (I) and (II) indicate alternate scans from which the difference spectra are computed. On the line rf the vertical bars labelled a and b stand for 90^{o} proton pulses, the grey shape in scheme (I) indicates the radio-frequency induced by the coupling of the solvent magnetization with the receiving circuit (radiation damping), and the box outlined by a broken line labelled {^{15}N} represents a ^{15}N filter used for artifact suppression. The box before acquisition represents the {^{15}N,^{1}H}-HSQC relay step performed with sensitivity enhancement (Fig. 27B) and water flip-back [88]. The relaxation delay τ_r is about 2.5 sec. On the line G, rectangles stand for gradient pulses. The duration of the gradients is typically 2 ms and they are applied with a strength of about 30 G/cm.

lock system have been set properly, and that possible small differences in the implementation of the relay step in alternate scans (for example, in the phase of potential water flip-back pulses) do not interfere with the proper performance [95]. These tests are necessary but not sufficient to ensure experiments free of artifacts. A successful presaturation test is not sufficient since presaturation suppresses the dipolar field and the radiation damping effects as well. In a further test a difference spectrum is measured without solvent saturation but with a very short mixing time of only a few milliseconds. In the resulting spectrum only exchange peaks should be detectable. If the solvent magnetization is in different "states" and therefore the demagnetizing field has different strength during evolution periods of two data sets to be subtracted, a difference NMR spectrum may contain “dispersive-like” artifacts [94], which are especially pronounced for narrow signals (Fig. 37B). Because phase cycling is a type of subtraction procedure, it alone can already produce such artifacts [265]. The artifacts created by radiation damping can be much more disturbing and are discussed in the next section.

5.4.3 Consequences of radiation damping and demagnetizing field effects

In this section the effects of radiation damping and demagnetising fields are analysed using the pulse sequence in Fig. 36. Fig. 37 shows spectra obtained with this scheme for a globular protein with 64 residues, a mutant form of the N-terminal domain of the 434-repressor which does not contain any hydroxyl groups [266]. A spectrum obtained without the ^{15}N filter (Fig. 36) contains signals for all amide protons in the protein except one, the position of which is indicated by a

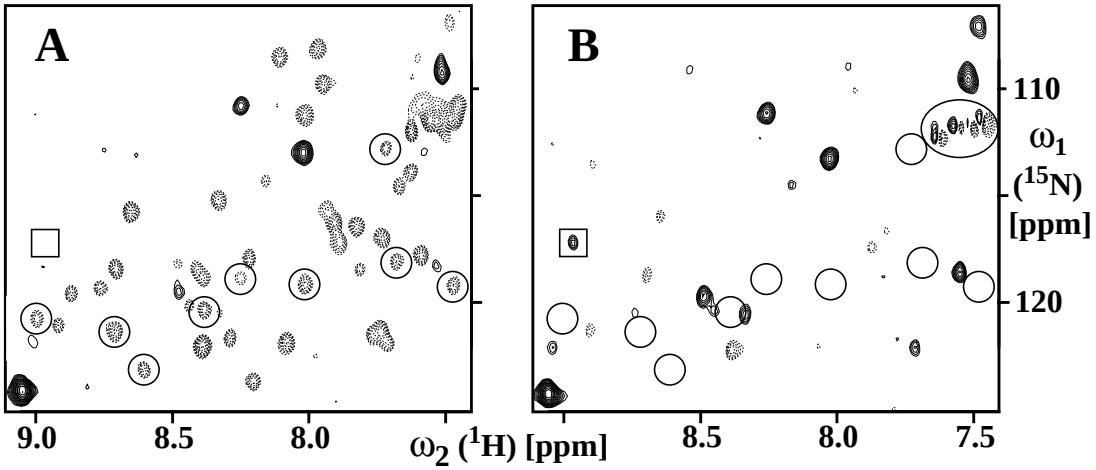

Fig. 37. Contour plots of expanded portions of two 2D {^{15}N,^{1}H}-HSQC-relayed NOE difference spectra measured with a 5 mM solution of a uniformly ^{15}N-labelled mutant form of the N-terminal DNA-binding domain of the 434 repressor. This mutant with 64 amino acids does not contain any hydroxyl groups. The solvent is 90% H_2O/10% D_2O, the pH 4.8 and the temperature 286 K. The spectrum was obtained with the sequence in Fig. 36, using τ_m = 68 ms. Negative peaks are drawn with dashed lines and positive peaks with solid lines. The circles mark cross peak positions that correspond to residues with less than 5% solvent accessibility. (A) The rectangle indicates the position of the only backbone amide signal that is missing when compared to a {^{15}N,^{1}H}-HSQC spectrum recorded with the same conditions. (B) Same as (A), except that a ^{15}N filter was inserted into the pulse sequence ({^{15}N} in Fig. 36). The ellipse indicates subtraction artifacts originating from the demagnetizing field effect.

square in Fig. 37. Such a result can hardly be expected for a globular protein with a well defined hydrophobic core that protects part of the amide protons from contacts with the solvent. A standard control 2D spectrum recorded with weak presaturation of the water resonance before the start of the actual pulse sequence contained no peaks. The pulse sequence in Fig. 36 uses radiation damping to select the water resonance. In the scheme radiation damping is included in the form of an induced shaped *rf* pulse. Radiation damping during an evolution period can be represented by a shaped pulse which is reminiscent of a truncated hyperbolic secant [263]. Such a shaped pulse can disturb the magnetization of spins that resonate as much as several kHz away from the solvent signal.

A systematic investigation of the phenomenon revealed that negative peaks are obtained for all resonances from an effect of the radiation damping field on the transverse component of the proton magnetization [95]. The negative peaks have intensities of the order of 1% of the equilibrium magnetization of the protein protons before the start of the pulse sequence. The artifacts in the spectrum of Fig. 37A can be eliminated by modifying the pulse sequence in such a way that there is no transverse magnetization for ^{15}N-bound protons during the mixing time τ_m. This can be achieved by addition of a ^{15}N filter [143, 267], as indicated in Fig. 36 with {^{15}N}. The modified experiment results in the spectrum shown in Fig. 37B. All cross peaks observed in the spectrum of Fig. 37B except possibly the ones framed by an ellipse (see below) correspond to amide protons of amino acid residues that are either at the protein surface or have the H^{α} chemical shift close to the water resonance. Interior amide protons (circles in Fig. 37) no longer show false NOEs to water protons. At the position indicated by a square in Fig. 37B, there is a weak positive

exchange peak, which was apparently cancelled in the spectrum of Fig. 37A by artifactual negative peak intensity.

The spectrum in Fig. 37B still contains “dispersive-like” peaks (framed by an ellipse) that originate from the effect of the demagnetizing field during acquisition. These peaks were masked by other strong artifacts in Fig. 37A. These “dispersive-like” peaks can be suppressed by omitting the water flip-back pulse in the {^{15}N,^{1}H}-HSQC relay step. Since the water magnetization at the end of the mixing period τ_m in the two experiments to be subtracted is either aligned along the positive *z* axis (scheme (I) in Fig. 36) or dephased (scheme (II)), the use of the water flip-back pulse in the {^{15}N,^{1}H}-HSQC relay step results in slightly different magnetic fields in the sample during acquisition. Similar “dispersive-like” patterns in the ^{15}N dimension are absent due to the averaging of the demagnetizing field effect achieved by the proton 180^{o} decoupling pulse in the middle of the ^{15}N evolution period, and the downscaling of the demagnetizing field effect by the smaller gyromagnetic ratio (Eq. (2.2)).

Other sequences used for hydration studies may produce similar artifacts when implemented on high field spectrometers. Another sequence for the detection of solvent–macromolecular NOEs that uses selective water flip-back based on radiation damping [246] shows similar artifacts which, however, cannot be suppressed simply with a ^{15}N filter [95]. Similarly an experimental scheme based on the application of selective pulses on the water resonance [243] contains peaks which do not show up in Fig. 37B.

In summary, many experiments designed to study hydration may suffer from artificial signals created by magnetic fields originating from the solvent magnetization. The intensity of these signals may be larger than the NOE peaks between hydration water molecules and protein protons. Pulse sequences for hydration measurements are very sensitive to small details in their implementation. Since test experiments with presaturation of the solvent signal eliminate radiation damping and the solvent demagnetizing field along with the artifacts arising from them, more extensive test procedures are required to ensure results which are free of artifacts. This becomes especially important when porting a pulse sequence to a spectrometer with a higher field, where radiation damping and demagnetizing field effects are intrinsically stronger.

In general, the test procedures for experiments designed for hydration studies should include a cancellation test for the relay step, a difference test with presaturation of the solvent signal, and an experiment with a very short mixing time (<5 ms). The demagnetizing field effect can be a source of “dispersive-like” subtraction artifacts which can usually be suppressed by proper modification of the pulse sequence to avoid different strength of the demagnetizing field in successive scans. The use of water flip-back pulses [88] seems especially attractive to increase the sensitivity but in some cases such pulses may have to be sacrificed for the sake of data reliability. In such situations the addition of a relaxation agent to obtain a faster relaxation of the water resonance may be a good compromise for measuring water–protein interactions [246].